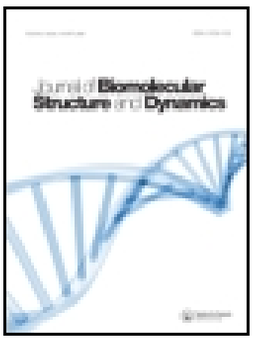

Taylor & Francis
Taylor & Francis Group

Journal of Biomolecular Structure and Dynamics

ISSN: 0739-1102 (Print) 1538-0254 (Online) Journal homepage: http://www.tandfonline.com/loi/tbsd20

Molecular dynamics simulations of lysozyme-lipid systems: probing the early steps of protein aggregation

Valeriya M. Trusova & Galyna P. Gorbenko

To cite this article: Valeriya M. Trusova & Galyna P. Gorbenko (2017): Molecular dynamics simulations of lysozyme-lipid systems: probing the early steps of protein aggregation, Journal of Biomolecular Structure and Dynamics, DOI: 10.1080/07391102.2017.1349691

To link to this article: http://dx.doi.org/10.1080/07391102.2017.1349691

Accepted author version posted online: 30 Jun 2017.

Publisher: Taylor & Francis

Journal: *Journal of Biomolecular Structure and Dynamics*

DOI: http://doi.org/10.1080/07391102.2017.1349691

Molecular dynamics simulations of lysozyme-lipid systems: probing the early steps of protein aggregation

Valeriya M. Trusova*, Galyna P. Gorbenko

Department of Nuclear and Medical Physics, V.N. Karazin Kharkov National University, 4 Svobody Sq., Kharkov 61022, Ukraine

*Address for correspondence:

Valeriya M. Trusova, 19-32 Geroyev Truda St., 61144 Kharkov, Ukraine

E-mail: valerija.trusova@karazin.ua

Tel.: +38 (057) 343 82 44

Molecular dynamics simulations of lysozyme-lipid systems: probing the early steps of protein aggregation

Using the molecular dynamics simulation, the role of lipids in the lysozyme transition into the aggregation-competent conformation has been clarified. Analysis of the changes of lysozyme secondary structure upon its interactions with the model bilayer membranes composed of phosphatidylcholine and its mixtures with phosphatidylglycerol (10, 40 and 80 mol%) within the time interval of 100 ns showed that lipid-bound protein is characterized by the increased content of β-structures. Along with this, the formation of protein-lipid complexes was accompanied by the increase of the gyration radius and the decrease in RMSD of polypeptide chain. The results obtained were interpreted in terms of the partial unfolding of lysozyme molecule on the lipid matrix, with the magnitude of this effect being increased with increasing the fraction of anionic lipids. Based on the results of molecular dynamics simulation, a hypothetical model of the nucleation of lysozyme amyloid fibrils in a membrane environment was suggested.

Keywords: hen egg white lysozyme, lipid bilayer, molecular dynamics, protein aggregation, amyloid

Introduction

One of the most remarkable features of protein molecules is their ability to form a diversity of supramolecular assemblies ranging from amorphous aggregates to the crystals with strictly defined translational symmetry in three directions (Buell, Dobson, & Knowles, 2014; Lee, Nam, Lee, Savelieff, & Lim, 2017). During the past decades, the process of one-dimensional crystallization of polypeptides resulting in the formation of highly-ordered fibrillar structures, called amyloids, receives ever growing attention (Trusova, 2015). Amyloid fibrils represent linear assemblies sharing a core cross-β-sheet structure and composed of monomeric subunits with translational symmetry in longitudinal direction (Adamcik, & Mezzenga, 2012; Chong et al. 2016). This class of protein aggregates is currently in the focus of extensive research efforts, since the formation of amyloid fibrils and their subsequent accumulation in different tissues and organs correlate with a wide range of debilitating disorders, including Parkinson's, Alzheimer's, Huntington's, Creutzfeld-Jakob diseases, type II diabetes, bovine spongiform encephalopathy, etc. (Chiti, & Dobson, 2006; Mezentsev et al., 2016, Alam et al., 2017, Ajmal et al., 2016). Furthermore, amyloids are regarded as prospective nanomaterials distinguished by superior physicochemical and mechanical properties, among which are high elasticity, rigidity, thermal and chemical stability, biocompatibility, etc. (Adamcik, & Mezzenga, 2012; Volpatti, & Knowles, 2014). It is becoming generally accepted that the main driving force for protein aggregation is partial unfolding of the native state of polypeptide chain into aggregation-prone conformation with exposed hydrophobic regions (Trusova, 2015). Ample evidence from both theoretical and experimental studies suggests that protein aggregation potential substantially enhances in a membrane environment (Gorbenko, & Trusova, 2012; Aisenbrey et al., 2008). Rapidly increasing number of reports indicates that protein association with lipid bilayers represents one of the principal processes which initiates the formation of

structurally-modified monomers and oligomers, evolving into the amyloid aggregates. It has been hypothesized that membrane disruption induced by early prefibrillar intermediates rather than mature fibrils, is the key pathway of amyloid toxicity (Gorbenko, & Kinnunen, 2006; Cao et al., 2013). Thus, the detailed understanding of the structure of protein oligomeric intermediates and molecular mechanisms of their formation is a major prerequisite for successful development of anti-amyloid strategies and timely prevention of conformational disorders (Ajmal et al., 2017). However, since these intermediates are transient and exist in a dynamic equilibrium with monomeric species, they can hardly be characterized at atomistic level by traditional biophysical techniques. In view of this, the methods of computer modeling are becoming widespread in the analysis of structural features of prefibrillar oligomers. Among these, the leading place belongs to the method of molecular dynamics (MD), a powerful tool in uncovering the precise mechanisms of conformational changes of biopolymers in solution and a membrane environment (Wei, Mousseau, & Derreumaux, 2007; Avila, Drechsel, Alcantara, & Viila-Freixa, 2011), protein folding and misfolding (Beck, & Daggett, 2004; Miao, Feixas, Eun, & McCammon, 2015), enzyme reactions (Bernardi, Cann, & Schulten, 2014), complexation of biomolecules (Hospital,Gorii, Orozco, & Gelpi, 2015), etc. Since the typical time scales for MD calculations range from nano- to microseconds, this method turned out to be extremely effective in the analysis of the early stages of polypeptide oligomerization. To exemplify, MD study of the structural peculiarities of $A\beta_{40}$ oligomers allowed the identification of the amino acid residues participating in the formation of β-sheets in amyloid aggregates (Urbanc et al., 2004). Based on the results of MD simulation, the lysozyme conformational states initiating the growth of fibrillar assemblies have been characterized (Kubiak-Ossowska, & Mulheran, 2011). The analysis of the trajectories of transthyretin intramolecular motion showed that the central fragment of the protein is responsible for its self-association, and

oligomeric aggregates have antiparallel structure (Paci, Gsponer, Salvatella, & Vendruscolo, 2004). MD simulations were proved to be informative in assessing the factors which weaken the amyloidogenic potential of the proteins. Specifically, Park et al. reported that polypeptide acidic region reduces the aggregation propensity of α-synuclein (Park et al., 2016). Likewise, it was shown that flavonoid derivative and small molecule inhibitor prevent the transition of Aβ and $A\beta_{42}$ peptides into oligomeric state (Shuaib & Goyal, 2016; Kumar et al., 2016).

In the present work, the molecular dynamics technique has been employed to gain insight into the role of a membrane environment in the formation of potentially amyloidogenic conformational intermediates of hen egg white lysozyme (HEWL). Amyloid fibrils from human lysozyme, that is highly homologous in structure to HEWL, are associated with familial nonneuropathic systemic amyloidosis, a disease in which pathological deposits are formed in liver, kidneys, and spleen (Frare, Mossuto, Polverino de Laureto, Dumoulin, Dobson, & Fontana, 2006; Alam et al., 2016). A good deal of studies have been devoted to the identification of lysozyme amyloidogenic fragments, and a number of structural models of the protein fibrillar aggregates have been suggested (Mossuto et al., 2010; Cao, Hu, & Lai, 2004). On the contrary, the molecular details of conformational transformation of lysozyme molecule in a membrane environment, underlying the protein transition in the aggregation-competent state, need further clarification. In the current study we made an attempt to fill this gap and concentrated our efforts on the investigation of the alterations in HEWL structure in the presence of lipid bilayers composed of zwitterionic lipid phosphatidylcholine (PC) and anionic lipid phosphatidylglycerol (PG) in different molar ratios. Remarkably, while choosing hen egg white lysozyme as a model protein in the present study, we proceed from the following advantageous features of this protein: i) well-characterized three-dimensional structure; ii) relatively small size, making the protein

suitable for computer simulations; iii) extensively studied routes and mechanisms of protein folding; iv) a wide range of conditions initiating/inhibiting the aggregation both *in vitro* and *in vivo*; v) high lipid-associating ability.

Molecular dynamics simulations

The molecular dynamics simulations were performed in GROMACS software (version 5.1) using the CHARMM36 force field. The calculations were done at a temperature of 310 K and a pressure of 1 bar. The crystal structure of HEWL (PDB ID: 1AKI) was used as a starting structure for simulations. The input files for MD calculations were prepared using web-based graphical interface CHARMM-GUI (Jo, Lim, Klauda, & Im, 2009). MD sumulations of HEWL-lipid systems were carried out in the NPT ensemble. The systems were fully hydrated and contained 185 lipid molecules and 8337 water molecules (total number of atoms was 51317). Hereafter, the systems containing 10, 40 or 80 mol% PG are referred to as PG10, PG40 and PG80, respectively.

The protein was solvated in an octahedron box with a minimum distance of 10 Å from the protein to the edge of the box. The TIP3P water model was used. To obtain a neutral total charge of the system a necessary number of counterions was added. For correct treatment of long-range electrostatic interactions, Particle Mesh Ewald algorithm (Darden, York, & Pedersen, 1993) was applied for long-range electrostatics and van der Waals cutoff was 10 Å. The pressure and temperature relaxation was set at 0.5 ps^{-1}. The minimization and equilibration of the system were performed during 50000 and 25000 steps, respectively. The time step for MD simulations was 2 fs. The trajectories and coordinates were saved every 2 ps for further analysis. The whole time interval for MD calculations was 100 ns. The commands *gmx rms, gmx rmsf, gmx gyrate* and *gmx sasa*, included in GROMACS, were used to calculate the RMSD, RMSF, R_g, and SASA.

The analysis of the hydration of individual amino acid residues was performed using

gmx trjorder command. The water molecule was identified as bound to the residue if the distance between oxygen atom of water and polar atom of amino acid residue was less than 2.8 Å. This distance is required for hydrogen bond to be formed (Blake, Pulford, & Artymuik, 1983; Roe, & Teeter, 1993). The output file generated after the performance of *gmx trjorder* command represents the number of water molecules within a shell of radius (< 2.8 Å) around the reference group (amino acid residue) as a function of time.

The evolution of the secondary structure was followed using the DSSP (Kabsch, & Sander, 1983) and VMD (Humphrey, Dalke, & Schulten, 1996) programs. Contact maps were generated using the CMView software (Vehlow, Stehr, Winkelmann, Duarte, Petzold, Dinse, & Lappe, 2011). Graphical representation of the protein was obtained using PyMOL.

Results

MD simulations have been performed for the two different orientations of HEWL with respect to the lipid/water interface (Figure 1). The orientation 1 (OR1) is based on the structural model of the lysozyme-lipid complexes described by Ibrahim et al., suggesting that specific helix-loop-helix domain (residues 87-114) accounts for the protein association with a lipid bilayer (Ibrahim, Thomas, & Pellegrini, 2001). The hydrophobic fragment of this domain (residues 87-95) inserts into the membrane nonpolar core, Arg112 and Arg114 form contacts with lipid headgroups, while Trp108 and Trp111 reside at the lipid/water interface. The orientation 2 (OR2) was obtained with the use of PPM server (Lomize, Pogozheva, Joo, Mosberg, & Lomize, 2012), which can predict the orientation of proteins within the membrane through minimizing the energy of protein transfer from aqueous to lipid phase. As illustrated in Figure. 1, according to PPM predictions the superficial position of HEWL molecule is the most energetically favorable.

Orientation 1. *Analysis of the radius of gyration and RMSD values.* At the first step of the study we investigated the effect of HEWL-lipid complexation on the overall stability of

protein molecule. Figure 2 represents the time course evolution of several structural parameters of HEWL associated with the lipid bilayers – the radius of gyration, the root-mean-square deviation and the solvent-accessible surface area. The radius of gyration (R_g) reflects the degree of protein structural compactness. Accordingly, the lower R_g corresponds to a more compact packing of polypeptide chain, while the higher R_g points to a more open protein structure. The analysis of the lysozyme radius of gyration in the free and membrane-bound states revealed that protein-lipid complexation is followed by the decrease in HEWL compactness due to its partial denaturation, the effect manifesting itself in the R_g increase from ~1.38 (solution) to ~1.41-1.43 nm (in the lipid bilayers) (Figure 2(a)).

Figure 2(b) shows the comparison of the backbone root-mean-square deviation (RMSD) for HEWL in the aqueous and lipid phases. It is clearly seen that the time required for attaining the equilibrium shortens upon the formation of protein-lipid complexes and decreases with the rise in the membrane surface potential. More specifically, in solution the RMSD value shows steady increase for the first 22 ns and afterwards fluctuates around average value (~0.21 nm). In turn, in the presence of lipid bilayers, the time for attaining a stable structure corresponds to 18, 13, 8 and 6 ns for PC, PG10, PG40 and PG80 bilayers, respectively. Along with this, the binding of lysozyme to lipids resulted in the decrease of the backbone RMSD. As seen from Figure 2(b), the RMSD value for the HEWL free in solution is ~0.21 nm, while in the presence of lipid bilayers this parameter ranges from ~0.13 to ~0.17 nm with the lowest value corresponding to the highest content of PG. The observed RMSD changes are most likely reflect the slowing of lysozyme intramolecular motion. Apparently, partial unfolding of the polypeptide chain on the lipid matrix leads to the rise in the protein surface area available for the contacts with the membrane and HEWL immobilization on the lipid bilayer that is followed by the decrease in RMSD.

Additional proofs in favor of this statement come from the analysis of the protein

solvent accessible solvent area (SASA). As shown in Figure 2(c), average values of SASA during 100 ns of simulation correspond to 66.2, 67.8, 70.4, 71.8 and 73.1 nm^2 for aqueous, PC, PG10, PG40 and PG80 systems, respectively. This indicates that lysozyme-membrane association is accompanied by the destabilization of the protein structure and exposure of the buried regions of polypeptide chain. Another interesting observation is the increase of SASA in the presence of lipid bilayers during the time of simulation. This effect may indicate that the process of the lysozyme partial unfolding on the lipid matrix is controlled by the time of protein-lipid interactions.

Evolution of lysozyme secondary structure. The lipid-induced changes in the secondary structure content of lysozyme are summarized in Table 1. When analyzing this Table, it is clearly seen that HEWL-lipid complexation is accompanied by the structural modifications of polypeptide chain, the magnitude of which depends on the molar fraction of PG. In the presence of lipids the protein structure is characterized by the increased content of extended β-strands, turns, coils and 3_{10}-helices (Tables 1 and 2) with the most significant changes implicating the β-stranded and 3_{10}-helical conformations. Accordingly, for lysozyme in solution the relative contributions of β-strands and 3_{10}-helix to the overall secondary structure were estimated to be 5.2 and 1.3%, respectively after 100 ns of MD simulations, while for the protein incorporated into PG80 membranes these values increase to 11.3 and 5.4%, respectively. Notably, the rise in the β-stranded and 3_{10}-helical structures occurs gradually with the elevation of PG molar fraction (Tables 1 and 2) and time of protein-lipid interactions, while the percentage of α-helix varies slightly. Interestingly, protein secondary structure was more stable in solution during the simulation as compared to the lipid-bound HEWL. To exemplify, the content of extended structures fluctuates around 5.2% for the free protein, while reaches the values 4.4, 4.7, 5.8 and 5.9% at 25, 50, 75 and 100 ns, respectively, in the presence of PC bilayers (Table 1). The same tendencies

were observed also for other examined systems and parameters.

In order to clarify, what amino acid residues are involved in the structural modifications of HEWL, we analyzed the time course of the changes in the protein secondary structure. The following effects have been revealed (Figure 3):

i) *the residues 64-65 and 78-79* – the unstructured regions (coils) are replaced with the extended β-sheet conformation. In the presence of neutral PC bilayer this conformation appears only after 50 ns of simulation, while the protein binding to the negatively charged membranes promotes the formation of β-sheets almost immediately;

ii) *the residues 79-83* – in solution and in the presence of PC membranes this protein fragment fluctuates between α- and 3_{10}-helix, while increasing the PG content results in the formation of stable 3_{10}-helix;

iii) *the residues 117-129* – the HEWL association with the lipid membranes is followed by the rise in the number of coils and turns, with the magnitude of this effect being increased with PG molar fraction;

iv) *the residues 17*-25 - 3_{10}-helix transforms into the two isolated bridges (i.e. formed from one pair of H-bonds of β-sheet) between the residues 19-20 and 23-24, with this effect being enhanced on elevating the PG concentration. Along with this, in PG80 membranes this bridge is replaced by β-sheet by the end of simulation (at ~90 ns).

All the above findings corroborate the results of R_g, RMSD and SASA analysis and suggest that the HEWL-lipid complexation gives rise to the formation of the protein aggregation-competent conformation, which is characterized by the destabilization of the HEWL native structure and the formation of β-structures being the major determinants of protein self-association.

The observed tendencies are reflected in the root-mean-square fluctuations (RMSF) of

C_α-atoms of the lysozyme residues. Figure 4 shows the comparison of RMSF for HEWL free in solution and bound to the lipid membranes. As can be judged from this figure, the RMSF of lysozyme in solution oscillates around 0.15 nm, while the lipid-associated protein displays the two-phase RMSF profile. Specifically, for the residues 1-110 the RMSF drops to average values of *ca.* 0.12, 0.09 and 0.05 nm for PC, PG40 and PG80 membranes, respectively, while for the residues 111-129 this quantity shows an increase as compared to solution. The decreased fluctuations of the lysozyme molecule in a lipid environment, revealed for the first 110 amino acid residues, may arise from the immobilization of the polypeptide chain within the lipid matrix due to the formation of protein-lipid contacts coupled with the slowing of the rotational and translational diffusion of the protein. This observation is in harmony with the results of RMSD calculations described above. In turn, the stronger fluctuations of the 111-129 residues correlate with the increased content of coils and turns in this region, suggesting that this fragment of polypeptide chain adopts more labile conformation upon the HEWL complexation with the lipid bilayers.

Analysis of the contact maps. A valuable information about the alterations in protein conformation may be obtained by analyzing the contact maps (CM). CM is defined as binary symmetric two-dimensional matrix with its non-zero elements representing the contacts between residues (Vendruscolo, & Domany, 1998). According to the generally accepted approach, two amino acid residues are considered as connected if they are spatially close with an 8.5 Å cutoff for the distance between their C_α-atoms (Bartoli, Capriotti, Fariselli, Martelli, & Casadio, 2008). Generally, four main characteristic patterns of secondary structure elements can be identified in CM: i) thick strips of contacts along the principal diagonal representing α-helices; ii) thin strips parallel to the principal diagonal illustrating parallel β-sheets; iii) thin cross-diagonal strips standing for antiparallel β-sheets; iv) small isolated clusters denoting loops, coils, etc.

Figure 5 depicts the set of contact maps of the HEWL in solution and in the presence of lipid bilayers. As seen from this figure, the protein-lipid interactions brought about the alterations in the network of the lysozyme intramolecular contacts. Notably, the magnitude of this effect gradually increased with the content of anionic lipid. The major modifications were found to occur in the two regions of polypeptide chain embracing the residues 60-81 and 103-129. Accordingly, the former fragment is characterized by the formation of new contacts between Arg61-Cys80, Trp63-Ile98, Tyr53-Cys80, Ser60-Leu84, Ile78-Ala90, etc. This phenomenon presumably relates to the ordering of 60-81 protein segment and appearance of the extended β-sheet conformation instead of the unstructured elements revealed by the secondary structure analysis (Figure 3). In turn, the HEWL embedment into the lipid bilayer is followed by the reduction of the number of the contacts in the latter protein fragment identified above (the residues 103-129). For instance, the break of contacts was found for the following pairs of residues: Asn106-Trp111, Cys115-Asp119, Met105-Arg112, Arg114-Gln121, pointing to the disruption of three-dimensional compactness of lysozyme due to the rise of turns and coils in this part of polypeptide chain (Figure 3). Importantly, the above sets of pairs are not exhaustive and given only for the sake of exemplification. The revealed tendencies reiterate the idea that in a membrane environment the lysozyme adopts a conformation of structurally-modified monomer with aggregation-prone regions.

In the following, it seems of interest to analyze how the conformation of Asp48/87/101 alters during the simulation since these residues are responsible for protein-lipid binding in OR1 or OR2. As indication of conformational changes, three parameters were chosen – RMSF, the angle between the main axes of the residue and membrane plane, θ, and number of water molecules bound to the residue, N_w. In order not to overload the present paper, in this kind of analysis we restricted ourselves only to the protein free in

aqueous solution and bound to PG80 lipid bilayers. The results obtained for OR1 are summarized in Table 3. RMSF for all three residues for HEWL in solution were found to fluctuate around average value without noticeable changes with time. In turn, protein incorporation into the lipid matrix in Orientation 1 resulted in the drop in RMSF of Asp48/87/101 with the magnitude of this effect being increased with the time of simulation. As was indicated above, the decreased values of RMSF may arise from the restriction of protein motion within the bilayer upon the formation of lysozyme-lipid contacts (Figures 2(b) and 4). Analogous tendencies were revealed upon examination of the degree of amino acid residue hydration. Specifically, all three examined Asp residues are in contact with 5-6 water molecules during the whole simulation for lysozyme free in solution. However, protein-lipid binding is accompanied by the reduction of Asp48/87/101 hydration (Table 3) up to ~1 water molecule per residue for Asp48 and ~2-3 water molecules per residue for Asp101 while Asp87 was found to be almost non-hydrated. Interestingly, the degree of residue hydration did not change significantly with the time of simulation. The decrease in the number of water molecules associated with Asp residues upon HEWL-lipid complexation may be explained by the protein transfer to the environment with the lower polarity. Contrary to N_w and RMSF, the angle θ showed the dependence on the time of MD simulation. Accordingly, increasing time of protein-lipid interactions was followed by the decrease in θ for Asp48/87/101, suggesting that the residues are tending to become parallel to the lipid bilayer surface. These observations coincide with the general conclusion about destabilization of HEWL structure upon complexation to lipid bilayers. Apparently, more labile conformation of the protein in a membrane environment may facilitate the rotation of amino acid residues.

Orientation 2. Contrary to OR1, the HEWL binding to the lipid bilayers in OR2 did not provoke profound alterations in the protein structure (Figure 6). Furthermore, no correlation

between the conformational reorganization of the lysozyme and the membrane surface potential has been found. Specifically, as it may be judged from Figure 6, the formation of β-sheets by the residues 64-65 and 78-79 in the presence of PC membranes was observed at ~45 ns of simulation while in the presence of PG40 and PG80 bilayers – at ~75 ns. In addition, the fragment embracing the residues 117-125 is characterized by the increased number of turns in the presence of PC, PG40 and PG80 membranes, however upon the HEWL association with PG10 bilayer the β-turn converts into α-helix. Finally, the radius of gyration and RMSD remain virtually unchanged upon the protein-lipid complexation (data not shown). These findings allow concluding that lysozyme insertion into bilayer interior is the necessary prerequisite for the protein transition in the aggregation-competent state.

Discussion

The results outlined in the previous section clearly show that lysozyme binding to the lipid membranes is accompanied by the increased content of β-structures and reduced structural stability of polypeptide chain. These processes represent the early stage of protein conversion from soluble monomeric to the insoluble aggregated form. Furthermore, structural modifications of the polypeptide chain were found to be regulated by the two main factors: i) the surface electrostatic potential of a lipid bilayer, and ii) the lysozyme disposition relative to the lipid-water interface, suggesting that both electrostatic and hydrophobic protein-lipid interactions contribute positively to the membrane-assisted HEWL transition to the transient state (Chaturvedi et al., 2016).

According to the generally accepted concept, the molecular basis for protein aggregation lies in the misfolding of polypeptide chain (Trusova, 2015). In general, under physiological conditions, polypeptide chain reaches its native functional state through the folding pathways. The process of protein folding is commonly described by the principle of minimal frustration (Onuchic, & Wolynes, 2004). According to this principle,

interdependent interactions between the side chain amino acid residues cooperatively lead to the most stable low-energy structure that is thus “minimally frustrated” (Plotkin, & Onuchic, 2000). This is reflected in the funnel-shaped energy landscape of a protein molecule which predicts that the free energy decreases while approaching to the native state. However, due to high conformational freedom and fluctuations, the funnel energy landscape of every protein molecule is rugged, displaying several additional local minima on the energy surface. This implies that at each step of the folding process, protein molecule is in an equilibrium with a partially folded intermediate, thereby reducing the probability of the polypeptide chain to reach its native state. The number and activity of such intermediates are controlled by polypeptide sequence and environmental conditions. These intermediate states generally have the exposed patches of hydrophobic amino acid residues which are prone to self-association. Hydrophobic interactions between partially folded states force the polypeptide chain to leave the native folding pathway and enter the off-folding route. Contrary to spontaneous and rapid folding process, the off-folding route is characterized by relatively slow kinetics. One of the possible off-folding pathways involves the transition of partially unfolded intermediates into the highly ordered fibrillar structures, amyloid fibers (Straub, J., & Thirumalai, 2011). These misfolded protein states are characterized by predominantly β-sheet secondary structure. The factors that shift the balance between the intramolecular forces accounting for correct protein packing, and trigger the off-folding transformation into the ordered self-assemblies involve genetic mutations, oxidative stress, environmental conditions (pH, temperature, ionic strength, pressure) and the binding to biological membranes. The main membrane-related factors initiating the protein transition into partially unfolded aggregation-competent state with the exposed nonpolar patches include: i) the changes in dielectric permittivity, ion concentration and pH at lipid/water interface compared to solution; ii) the interaction of polypeptide with electric field created

by the charged lipid groups, phosphocholine dipoles and the dipoles of bound water; iii) the formation of ionic contacts with specific lipid groups. Protein folding in a lipid phase differs from that in solution since nonpolar lipid groups compete with nonpolar protein groups for hydrophobic interactions. The transfer of the exposed hydrophobic regions from an aqueous to a lipid phase yields the energy gain required for the subsequent polypeptide oligomerization. In addition, due to nonuniform surface distribution of the charged amino acid residues, protein molecule specifically orients in the membrane electric field to minimize the electrostatic binding energy. All these considerations provide a basis for explanation of the HEWL tendency to adopt the aggregation-competent conformation upon its association with lipid bilayers in OR1 revealed by the molecular dynamics simulation.

It should be noted that although the results presented here cannot be directly transferred to the lysozyme fibrillization *in vivo*, they still provide valuable insights into the protein amyloidogenesis. Specifically, some ideas concerning the possible structure of amyloid fibrils formed on a lipid matrix may be formulated. Based on the results of infrared spectroscopy, it has been shown that protein conformers possessing 3_{10}-helix and β-turns represent the intermediate between the native and aggregated protein (Dong, A., Randolph, T., & Carpenter, 2000). In addition, according to our hypothesis, one of the possible aggregation route of HEWL involves the transition α-helix→3_{10}-helix→β-structure. The revealed transition of the residues 64-65 and 78-79 into β-conformation suggests that they display the highest aggregation potential in a membrane environment. Apparently, these residues reside in the core of lysozyme amyloid fibrils through which the central fibril axis passes. Since the above pairs of residues are separated by the turns, one may suppose that lysozyme fibrillar aggregates growing on the membrane have the structure of steric zipper in which β-sheets formed by the residues 64-65 and 78-79, are in a complementary position (Figure 7). Additional stabilization of the fibril seems to be provided by the β-bridges in the

HEWL N-terminal segment (the residues 19-20 and 23-24) as well as by the β-turns and unstructured fragments localized in the C-terminal protein region (the residues 117-129). Furthermore, it seems likely that in the mature fibril β-sheets have more extended structure and embrace the residues Gly54-Asn65 and Ile78-Thr89 (Figure 7). This assumption is based on the results of the prediction of lysozyme fragments with the highest aggregation propensity implemented by the eight web-algorithms, including Pasta2, AmylPred2, Tango, MetAmyl, Waltz, Aggrescan, BetaScan та FoldAmyloid (Trusova, 2016). Briefly, the fragment was identified as amyloidogenic if it was predicted by at least four algorithms. It appeared that HEWL is characterized by the five aggregation-prone regions which embrace the following residues: 27-31 (NWVCA), 53-60 (YGILQINS), 81-90 (SALLSSDITA), 106-110 (NAWVA) and 121-125 (QAWIR) with the highest amyloidogenic potential being recovered for the second and third fragments. Notably, the analysis of the secondary structure evolution profiles (Figure 3) revealed that the residues 78-89 are in 3_{10}-helical and unstructured conformation. However, as it was mentioned above, 3_{10}-helix and unstructured conformations may represent the intermediate states for β-sheet, thus it is likely that this fragment of polypeptide chain would adopt β-conformation but the time needed for such conformational transition exceeds the time of simulation (100 ns). Importantly, since the main idea of the present study was to demonstrate the principal possibility for the transition of the lipid-associated HEWL into aggregation-competent conformation, but not the description of the whole process of protein fibrillization, the proposed model of the nucleation of lysozyme amyloid fibrils in a membrane environment is hypothetical and based on some assumptions described above. Intriguingly, this model is in good harmony with the model of Tokunaga et al. who showed that the residues 54-62 represent the hydrophobic core of the HEWL fibrils (Tokunaga, Y., Sakakibara, Y., Kamada, Y., Watanabe, K., & Sugimoto, 2013). On the other hand, according to the hypothesis of Krebs

and co-authors, protein fragment participating in the fibrillization involves the residues 49-64 (Krebs et al., 2000), while Frare et al. reported that lysozyme amyloidogenic region is more extended and embraces the residues 32-108 (Frare, Mossuto, Polverino de Laureto, Dumoulin, Dobson, & Fontana, 2006). It is worth of noting that these data were obtained for protein fibrils growing in solution. Apparently, nucleation on the lipid matrix would result in a different final conformation of the fibrillar aggregates. In this aspect special attention should be given to the role of the C-terminal fragment of HEWL (the residues 117-129) which is characterized by the increase in the degree of disordering upon the protein-membrane binding. Previously it was shown that structural polymorphism of the lysozyme amyloid fibrils plays a crucial role in their cytotoxicity. Accordingly, fibrillar aggregates with the smaller size of the central ordered core and the higher content of turns and unstructured elements displayed a more pronounced cytotoxic activity compared to the fibrils with almost the whole polypeptide chain being in β-conformation (Mossuto et al., 2010). As the most probable reason for this effect the authors considered a high membranotropic activity of the unstructured protein fragments. It is supposed that the regions of polypeptide chain residing outside the fibril core represent the major binding sites for membrane interactions. The labile unstructured or turn conformation of these protein segments facilitates their effective association with the lipid bilayer. Obviously, analogous processes take place in the systems examined here. It seems likely that the HEWL fragment involving the residues 117-129 binds to the membrane and anchor the whole fiber on the lipid matrix. The validity of this assumption is corroborated by the high hydrophobicity of this fragment favoring its incorporation into lipid bilayer. At the same time, the above segment contains several charged residues that may form contacts with lipid headgroups. All these considerations allow concluding that the fragment 117-129 is located at the interphase between polar and nonpolar membrane parts. Importantly, the described model of the

lysozyme amyloid assemblies growing on the lipid matrix is in agreement with the results of our previous experimental study showing that membranotropic activity of fibrillar lysozyme is directed mainly at the surface layer of the membrane (Kastorna, A., Trusova, V., Gorbenko, G., & Kinnunen, 2012).

Conclusions

Cumulatively, the molecular dynamics simulations have been performed to uncover the role of a lipid environment in the transition of hen egg white lysozyme into the aggregation-competent conformation. The analysis of several structural parameters derived from the simulations, along with the examination of the protein secondary structure profiles and contact maps, showed that the HEWL association with the lipid bilayers from phosphatidylcholine and its mixtures with 10, 40 or 80 mol % of phosphatidylglycerol is followed by the formation of conformationally-modified protein monomers, the process manifesting itself in the increase of the β-structure content and partial unfolding of polypeptide chain. This effect was found to be dependent on the molar fraction of anionic lipid and protein orientation with respect to the lipid/water interface highlighting the important role of both electrostatic and hydrophobic protein-lipid interactions in controlling the lysozyme structural transitions. The results obtained seem to be of utmost importance in the context of lysozyme amyloidogenesis, since timely detection of early steps of protein aggregation and self-association into critical oligomeric nucleus is a necessary prerequisite for prevention of the conformational disorders and development of novel anti-amyloid strategies.

References

Adamcik, J., & Mezzenga, R. (2012). Protein fibrils from a polymer physics perspective. *Macromolecules*, 45, 1137-1150.

Ajmal, M., Nusrat, S., Alam, P., Zaidi, N., Badr, G., …, & Khan, R. (2016). Differential

mode of interaction of Thioflavin T with native β structural motif in human α 1-acid glycoprotein and cross beta sheet of its amyloid: biophysical and molecular docking approach. *Journal of Molecular Structure*, 117, 208-217.

Ajmal, M., Chaturvedi, S., Zaidi, N., Alam, P., Zaman, M., …, & Khan, R. (2017). Biophysical insights into the interaction of hen egg white lysozyme with therapeutic dye clofazimine: modulation of activity and SDS induced aggregation of model protein. *Journal of Biomolecular Structure and Dynamics*, 35, 2197-2210.

Aisenbrey, C., Borowik, T., Bystrom, R., Bokvist, M., Lindstrom, F., … Grobner, G. (2008). How is protein aggregation in amyloidogenic diseases modulated by biological membranes? *European Biophysics Journal*, 37, 247-255.

Alam, P., Chaturvedi, S., Siddiqi, M., Rajpoot, R., Ajmal, M., …, & Khan, R. (2016). Vitamin k3 in inhibits protein aggregation: implication in the treatment of amyloid diseases. *Scientific Reports*, 6, 26759-26769.

Alam, P., Beg, A., Siddiqi, M., Chaturvedi, S., Rajpoot, R., …, & Khan, R. (2017). Ascorbic acid inhibits human insulin aggregation and protects against amyloid induced cytotoxicity. *Archives of Biochemistry and Biophysics*, 621, 54-62.

Avila, C., Drechsel, N., Alcantara, R., & Viila-Freixa, J. (2011). Multiscale molecular dynamics of protein aggregation. *Current Protein & Peptide Science*, 12, 221-234.

Bartoli, L., Capriotti, E., Fariselli, P., Martelli, P., & Casadio, R. (2008). The pros and cons of predicting protein contact maps. *Methods in Molecular Biology*, 413, 199-217.

Beck, D., & Daggett, V. (2004). Methods for molecular dynamics simulations of protein folding/unfolding in solution. *Methods*, 34, 112-120.

Bernardi, R., Cann, I., & Schulten, K. (2014). Molecular dynamics study of enhanced Man5B enzymatic activity. *Biotechnology for Biofuels*, 7, 83-90.

Blake, C., Pulford, W., & Artymuik, P. (1983). X-ray study of water in crystals of lysozyme.

Journal of Molecular Biology, 167, 693-723.

Buell, K., Dobson C., & Knowles T. (2014). The physical chemistry of the amyloid phenomenon: thermodynamics and kinetics of filamentous protein aggregation. *Essays of Biochemistry*, 56, 11-39.

Cao, P., Abedini, A., Wang, H., Tu, L., Zhang, X., Schmidt, A., Raleig, D. (2013). Islet amyloid polypeptide toxicity and membrane interactions. *Proceedings of the National Academy of Sciences of the United States of America*, 110, 19279-19284.

Cao, A., Hu, D., & Lai, L. (2004). Formation of amyloid fibrils from fully reduced hen egg white lysozyme. *Protein Science*, 13, 319-324.

Chaturvedi, S., Khan, J., Siddiqui, M., Alam, P., & Khan, R. (2016). Comparative insight into surfactants mediated amyloidogenesis of lysozyme. *International Journal of Biological Macromolecules*, 83, 315-325.

Chiti, F, Dobson, C. (2006). Protein misfolding, functional amyloid and human diseases. *Annual Reviews of Biochemistry*, 75, 333-366.

Chong, X., Lu, X., Wang, Y., Chang, A., Xu, L., … He J. (2016). Distinct structural changes in wild-type and amyloidogenic chicken cystatin caused by disruption of C95-C115 disulfide bond. *Journal of Biomolecular Structure and Dynamics*, 34, 2679-2687.

Darden, T., York, D., & Pedersen, L. (1993). Particle mesh Ewald: an $N\cdot\log(N)$ method for Ewald sums in large systems. *Journal of Chemical Physics*, 98, 10089-10092.

Dong, A., Randolph, T., & Carpenter, J. (2000). Entrapping intermediates of thermal aggregation in α-helical properties with low concentration of guanidine hydrochloride. *Journal of Biological Chemistry*, 275, 27689-27693.

Frare, E., Mossuto, M., Polverino de Laureto, P., Dumoulin, M., Dobson, C., & Fontana, A. (2006). Identification of the core structure of lysozyme amyloid fibrils by proteolysis. *Journal of Molecular Biology*, 361, 551-561.

Gorbenko, G., & Kinnunen, P. (2006). The role of lipid-protein interactions in amyloid-type protein fibril formation. *Chemistry and Physics of Lipids*, 141, 72-82.

Gorbenko, G., & Trusova, V. (2012). Protein aggregation in a membrane environment. *Advances in Protein Chemistry and Structural Biology*, 84, 114-152.

Hospital, A., Gorii, J., Orozco, M., & Gelpi, J. (2015). Molecular dynamics simulations: advances and applications. *Advances and Applications in Bioinformatics and Chemistry*, 8, 37-47.

Humphrey, W., Dalke, A., & Schulten, K. (1996). VMD – Visual Molecular Dynamics. *Journal of Molecular Graphics*, 14, 33-38.

Ibrahim, H., Thomas, U., & Pellegrini, A. (2001). A helix-loop-helix peptide at the upper lip of the active site cleft of lysozyme confers potent antimicrobial activity with membrane permeabilization action. *Journal of Biological Chemistry*, 276, 43767-43774.

Jo, S., Lim J., Klauda, J., & Im, W. (2009). CHARMM-GUI membrane builder for mixed bilayers and its application to yeast membranes. *Biophysical Journal*, 97, 50-58.

Kabsch, W., & Sander, C. (1983). Dictionary of protein secondary structure: pattern recognition of hydrogen-bonded and geometrical features. *Biopolymers*, 22, 2577-2637.

Kastorna, A., Trusova, V., Gorbenko, G., & Kinnunen, P. (2012). Membrane effects of lysozyme amyloid fibrils. *Chemistry and Physics of Lipids*, 165, 331-337.

Krebs, M., Wilkins, D., Chung, E., Pitkeathly, M., Chamberlain, A., Zurdo, J., … Dobson, C. (2000). Formation and seeding of amyloid fibrils from wild-type hen lysozyme and a peptide fragment from the β-domain. *Journal of Molecular Biology*, 300, 541-549.

Kubiak-Ossowska, K., & Mulheran, P. (2011). Multiprotein interactions during surface adsorption: a molecular dynamics study of lysozyme aggregation at a charged solid surface. *Journal of Physical Chemistry B*, 115, 8891-8900.

Kumar, A., Srivastava, S., Tripathi, S., Singh, S., Srikrishna, S., & Sharma, A. (2016).

Molecular insights into amyloid oligomer destabilizing mechanism of flavonoid derivative 2-(4' benzyloxyphenyl)-3-hydroxy-chromen-4-one through docking and molecular dynamics simulations. *Journal of Biomolecular Structure and Dynamics*, 34, 1252-1263.

Lee S.J.C., Nam E., Lee H.J., Savelieff M.G., & Lim, M.H. (2017). Towards an understanding of amyloid-β oligomers: characterization, toxicity mechanisms, and inhibitors. *Chemical Society Reviews*, 46, 310-323.

Lomize, M., Pogozheva, I., Joo, H., Mosberg, H., & Lomize, A. (2012). OPM database and PPM web server: resources for positioning of proteins in membranes. *Nucleic Acid Research*, 40, D370-D376.

Mezentsev, Y., Medvedev, A., Kechko, O., Makarov, A., Ivanov, A., … Kozin, S. (2016). Zinc-induced heterodimer formation between metal-binding domains of intact and naturally modified amyloid-beta species: implication to amyloid seeding in Alzheimer's disease? *Journal of Biomolecular Structure and Dynamics*, 34, 2317-2326.

Miao, Y., Feixas, F., Eun, C., & McCammon, J.A. (2015). Accelerated molecular dynamics simulations of protein folding. *Journal of Computational Chemistry*, 36, 1536-1549.

Mossuto, M., Dhulesia, A., Devlin, G., Frare, E., Kumita, J., Polverino de Laureto, P., … Salvatella, X. (2010). The non-core regions of human lysozyme amyloid fibrils influence cytotoxicity. *Journal of Molecular Biology*, 402, 783-796.

Onuchic, J., & Wolynes, P. (2004). The theory of protein folding. *Current Opinion in Structural Biology*, 14, 70-75.

Paci, E., Gsponer, J., Salvatella, X., & Vendruscolo, M. (2004). Molecular dynamics studies of the process of amyloid aggregation of peptide fragments of transthyretin. *Journal of Molecular Biology*, 340, 555-569.

Park, S., Yoon, J., Jang, S., Lee K., & Shin, S. (2016) The role of acidic domain of α-synuclein in amyloid fibril formation: a molecular dynamics study. *Journal of Biomolecular*

Structure and Dynamics, 34, 376-383.

Plotkin, S., & Onuchic, J. (2000). Investigation of routes and funnels in protein folding by free energy functional methods. *Proceedings of the National Academy of Sciences of the United States of America*, 97, 6509-6514.

Roe, S., & Teeter, M. (1993). Patterns for prediction of hydration around polar residues in proteins. *Journal of Molecular Biology*, 229, 419-427.

Shuaib, S. & Goyal, B. (2017). Scrutiny of the mechanism of small molecule inhibitor preventing conformational transition of amyloid-β_{42} monomer: insights from molecular dynamics simulations. *Journal of Biomolecular Structure and Dynamics*, doi: 10.1080/07391102.2017.1291363.

Straub, J., & Thirumalai, D. (2011). Towards a molecular theory of early and late events in monomer to amyloid fibril formation. *Annual Reviews in Physical Chemistry*, 62, 437-463.

Tokunaga, Y., Sakakibara, Y., Kamada, Y., Watanabe, K., & Sugimoto, Y. (2013). Analysis of core region from egg white lysozyme forming amyloid fibrils. *International Journal of Biological Sciences*, 9, 219-227.

Trusova, V. (2015). Protein fibrillar nanopolymers: molecular-level insights into their structural, physical and mechanical properties. *Biophysical Reviews and Letters*, 10, 135-156.

Trusova, V. (2016). Theoretical analysis of amyloidogenic potential of lysozyme, cytochrome *c* and apolipoprotein A-I. *Biophysical Bulletin*, 36, 5-10.

Urbanc, B., Cruz, L., Ding, F., Sammond, D., Khare, S., Buldyrev, S., … Dokholyan, N. (2004). Molecular simulations of amyloid β dimer formation. *Biophysical Journal*, 87, 2310-2321.

Vehlow, C., Stehr, H., Winkelmann, M., Duarte, J., Petzold, L., Dinse, J., & Lappe, M. (2011). CMView: interactive contact map visualization and analysis. *Bioinformatics*, 27,

1573-1574.

Vendruscolo, M., & Domany, E. (1998). Efficient dynamics in the space of contact maps. *Folding & Design*, 3, 329-336.

Volpatti, L., & Knowles, T. (2014). Polymer physics inspired approaches for the study of the mechanical properties of amyloid fibrils. *Journal of Polymer Science A*, 52, 281-292.

Wei, G., Mousseau, N., Derreumaux, P. (2007). Computational simulations of early steps of protein aggregation. *Prion*, 1, 3-8.

Legends to Figures

Figure 1. Two types of lysozyme orientation in membrane used for molecular dynamics simulations

Figure 2. Time course evolution of HEWL structural parameters in different systems: radius of gyration (A), root-mean-square deviation (B) and solvent-accessible surface area (C). Different colors of the curves stand for HEWL free in solution (black) or bound to PC (red), PG10 (blue), PG40 (pink) and PG80 (green) lipid bilayers.

Figure 3. Changes in HEWL secondary structure during 100 ns MD simulation in solution (A) or upon protein association with PC (B), PG10 (C), PG40 (D) and PG80 (E) lipid bilayers in Orientation 1. Color codes of HEWL secondary structure denote: **T** – turn, **E** – extended structure, **B** – isolated β-bridge, **H** – α-helix, **G** – 3_{10}-helix, **I** – π-helix, **C** – coil.

Figure 4. HEWL root-mean square fluctuations as a function of residue number.

Figure 5. Residue-residue contact maps of HEWL in solution and in lipid bilayers of different composition. Big and small blue ovals represent the regions of polypeptide chain embracing the residues Ser60-Ser81 and Asn103-Leu129, respectively. The right bottom panel depicts the HEWL structure with identified regions.

Figure 6. Time course evolution of HEWL secondary structure upon binding to PC (A), PG40 (B) or PG80 (C) lipid bilayers in Orientation 2.

Figure 7. Hypothetical model of HEWL amyloid fibrils formed in membrane environment.

Table 1. Secondary structure content of HEWL in solution and bound to PC lipid bilayers

	Solution				**PC**			
	25 ns	50 ns	75 ns	100 ns	25 ns	50 ns	75 ns	100 ns
α-helix	33.6	33.2	33.8	33.9	33.4	33.6	33.9	33.9
3_{10}-helix	1.1	1.3	1.2	1.3	1.4	1.3	1.6	1.4
π-helix	-	-	-	-	-	-	-	-
Extended strand	5.4	5.2	5.3	5.2	4.4	4.7	5.8	5.9
Turn	14.1	14.5	14.7	14.7	15.0	15.0	15.0	15.0
Bend	26.5	26.6	26.6	26.6	24.7	24.6	24.6	24.6
Coil	14.7	15.0	15.2	15.2	15.4	15.7	16.0	16.1
Isolated β-bridge	3.1	3.1	3.1	3.1	3.1	3.1	3.1	3.1

Table 2. Secondary structure content of HEWL in the presence of PC/PG lipid bilayers

	PG10				**PG40**				**PG80**			
	25 ns	50 ns	75 ns	100 ns	25 ns	50 ns	75 ns	100 ns	25 ns	50 ns	75 ns	100 ns
α-helix	34.2	34.2	34.1	34.2	34.6	34.3	34.6	34.6	34.3	34.6	34.9	34.9
3_{10}-helix	3.1	3.5	3.7	3.7	4.1	4.4	4.4	4.4	5.1	5.3	5.4	5.4
π-helix	-	-	-	-	-	-	-	-	-	-	-	-
Extended strand	8.6	9.1	9.2	9.2	9.3	9.7	10.5	10.8	10.6	11.3	11.2	11.3
Turn	16.9	16.8	16.6	16.6	20.1	20.1	19.4	19.2	20.7	20.9	21.0	21.0
Bend	13.9	13.9	13.9	13.9	7.2	7.2	7.2	7.2	2.3	2.4	2.4	2.4
Coil	19.2	19.4	19.4	19.3	19.4	19.5	20.7	20.7	21.4	21.0	21.7	21.9
Isolated β-bridge	3.1	3.1	3.1	3.1	3.1	3.1	3.1	3.1	3.1	3.1	3.1	3.1

Table 3. Structural parameters and hydration of Asp48, Asp87 and Asp101 of HEWL free in solution or bound to PG80 lipid bilayers in Orientation 1

		N_w				RMSF, nm				θ, °			
		25 ns	50 ns	75 ns	100 ns	25 ns	50 ns	75 ns	100 ns	25 ns	50 ns	75 ns	100 ns
Asp48	solution	6.1	5.9	5.7	5.4	0.27	0.29	0.28	0.29	-	-	-	-
	PG80	1.2	0.7	1.0	1.5	0.31	0.25	0.19	0.14	52	47	41	36
Asp87	solution	6.0	6.2	5.4	5.8	0.15	0.16	0.15	0.13	-	-	-	-
	PG80	0.9	0.8	0.9	0.7	0.15	0.14	0.11	0.09	44	44	33	31
Asp101	solution	5.7	6.2	6.2	5.9	0.21	0.22	0.22	0.22	-	-	-	-
	PG80	2.2	2.1	2.9	2.3	0.21	0.19	0.15	0.12	28	22	17	14

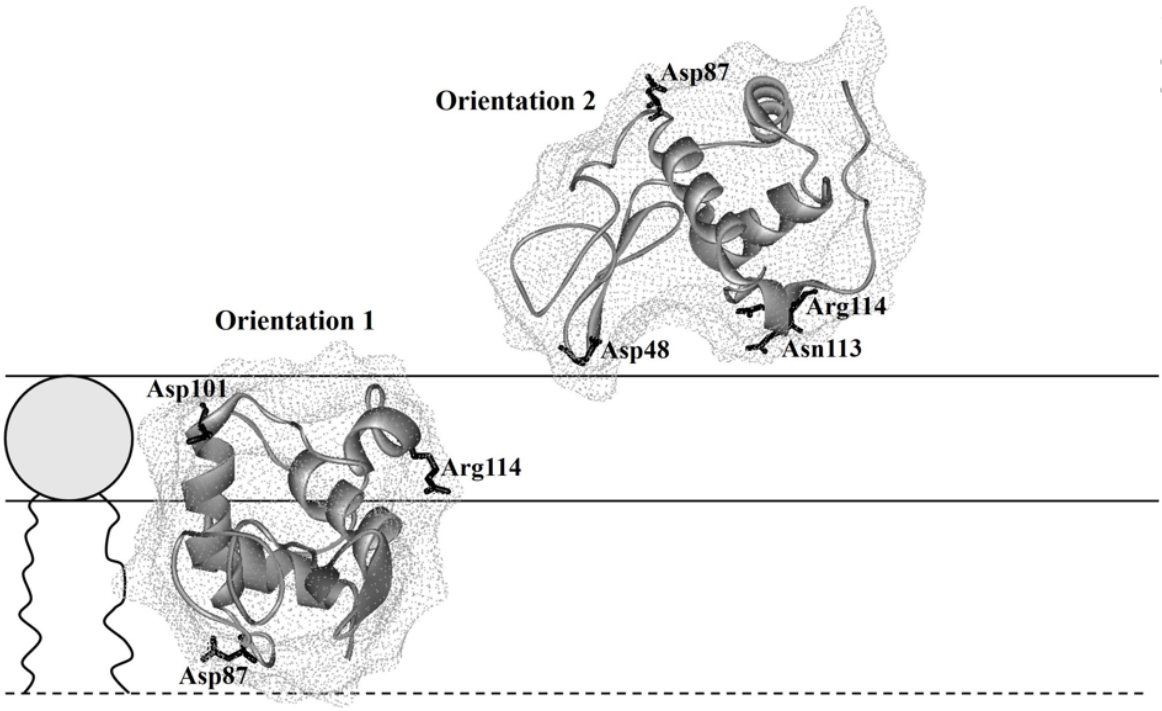
Orientation 2
Asp87
Arg114
Asn113
Asp48
Orientation 1
Asp101
Arg114
Asp87

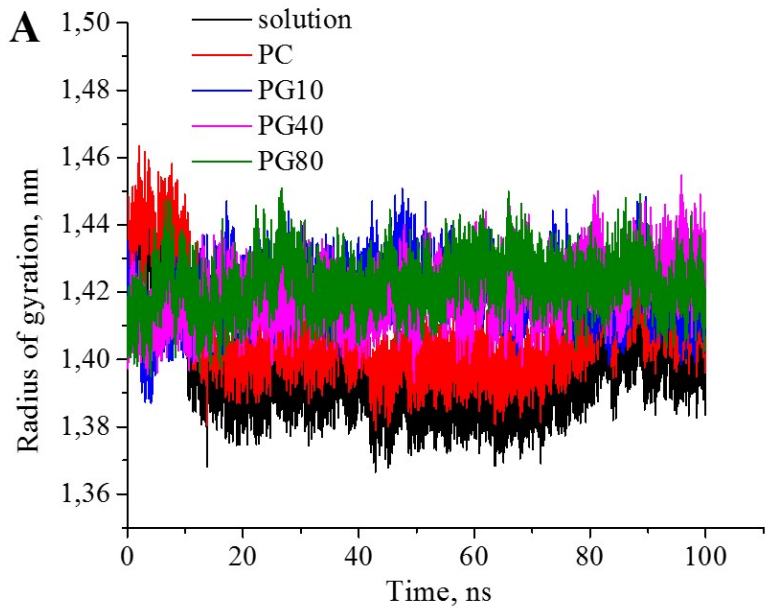

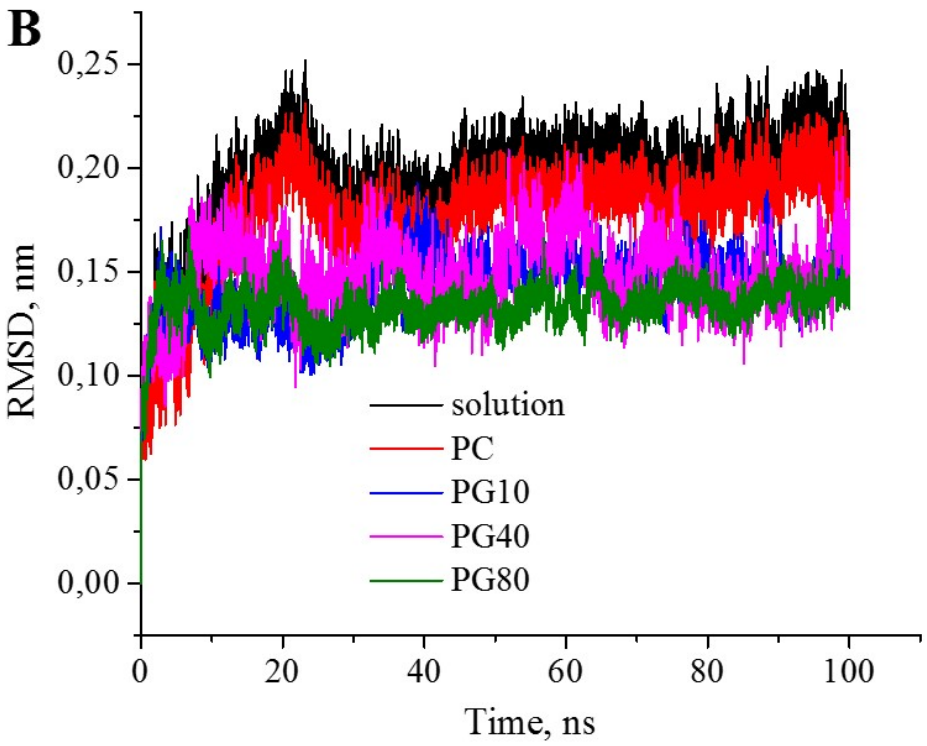

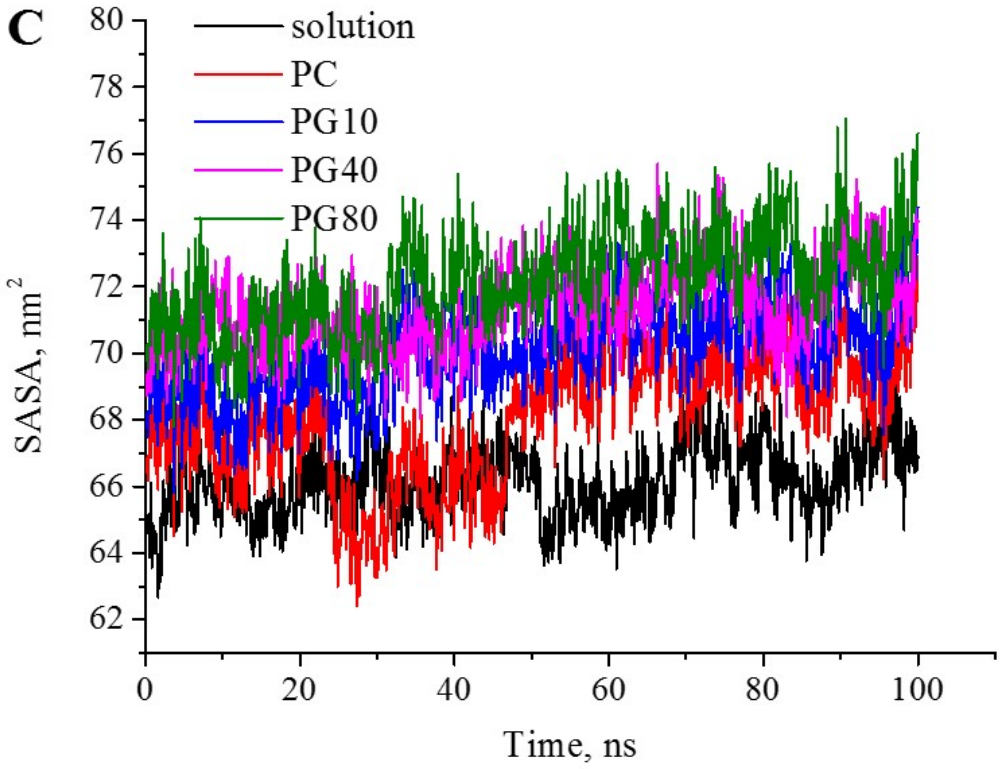
C
solution
PC
PG10
PG40
PG80
SASA, nm^2
Time, ns
80
78
76
74
72
70
68
66
64
62
0
20
40
60
80
100

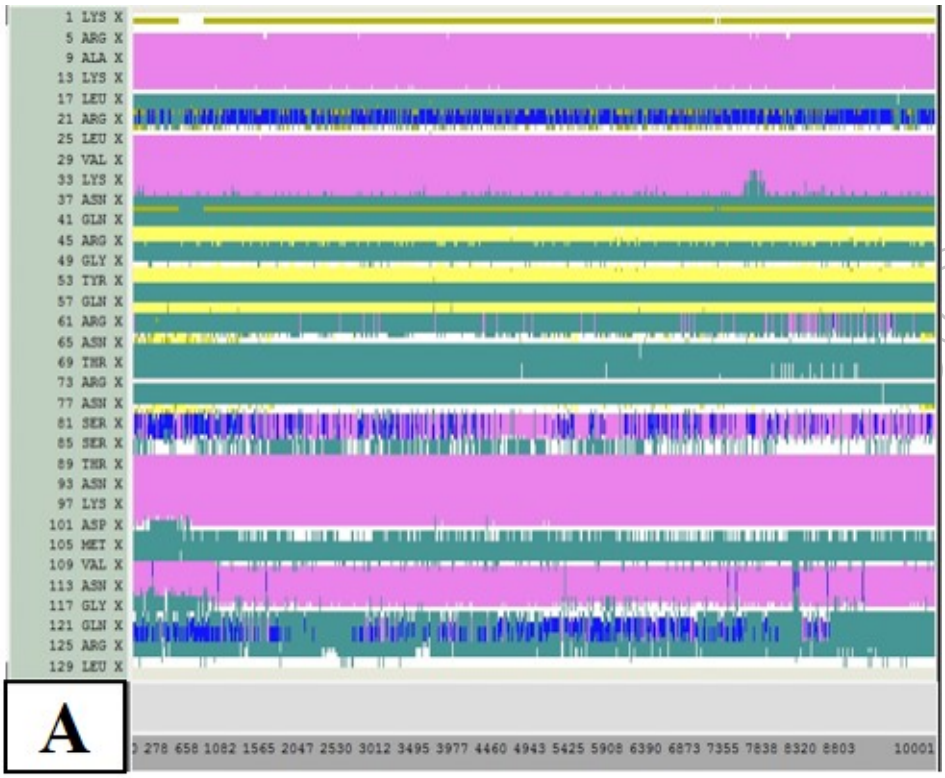

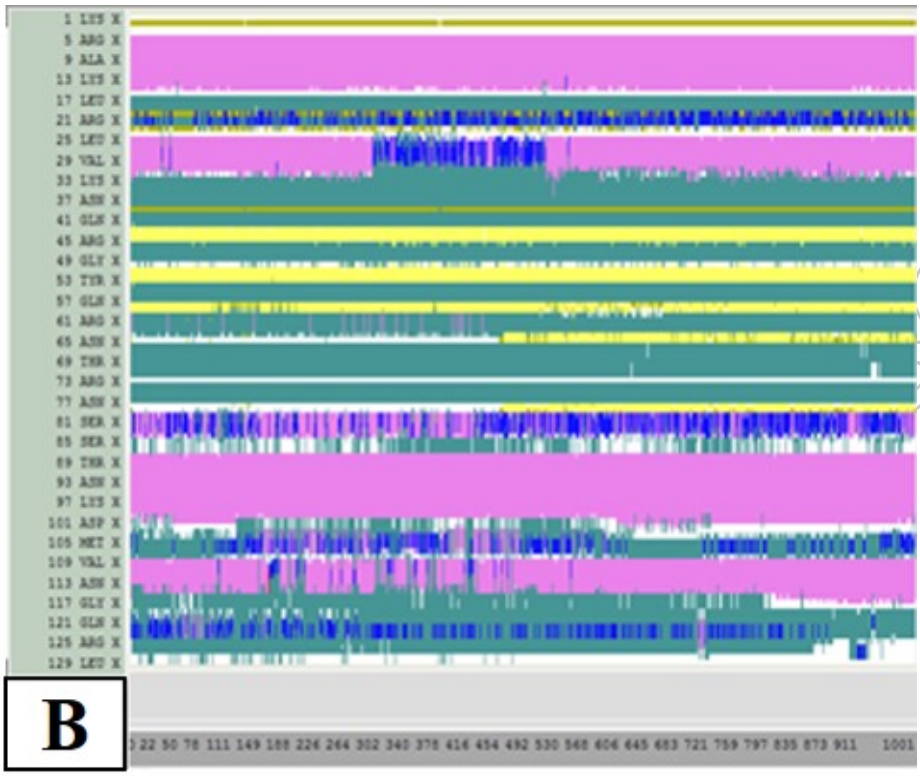

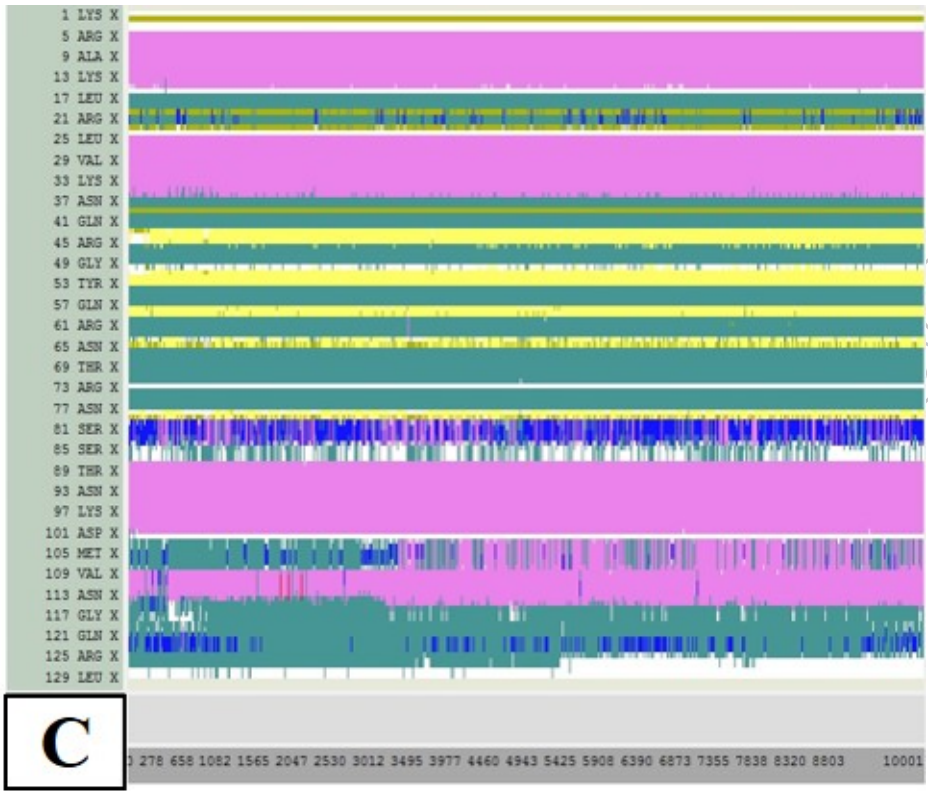

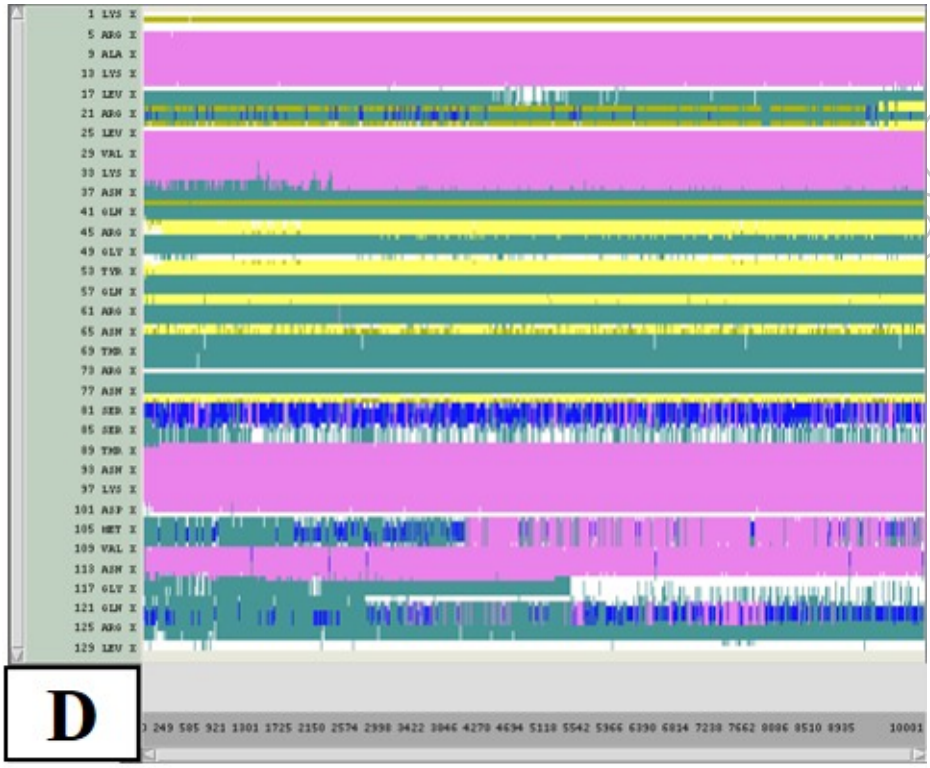

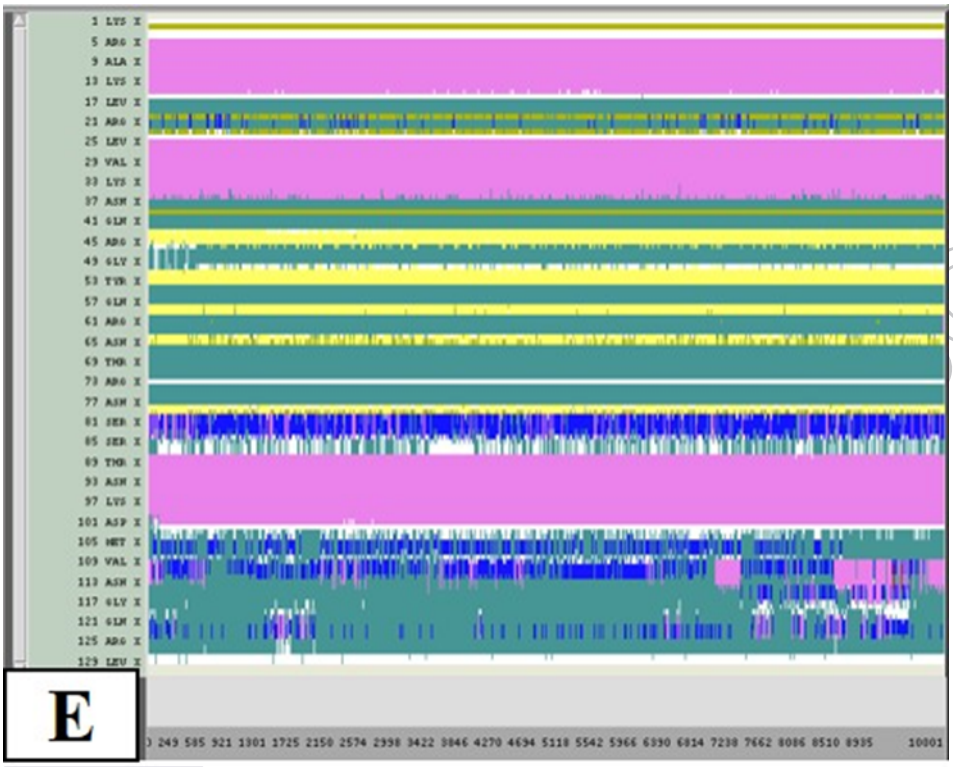

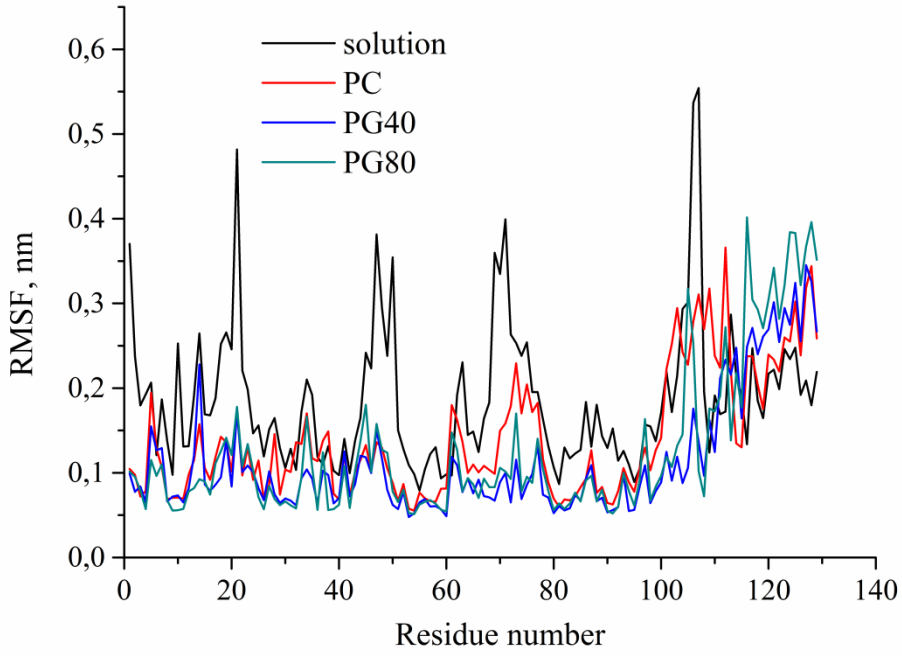

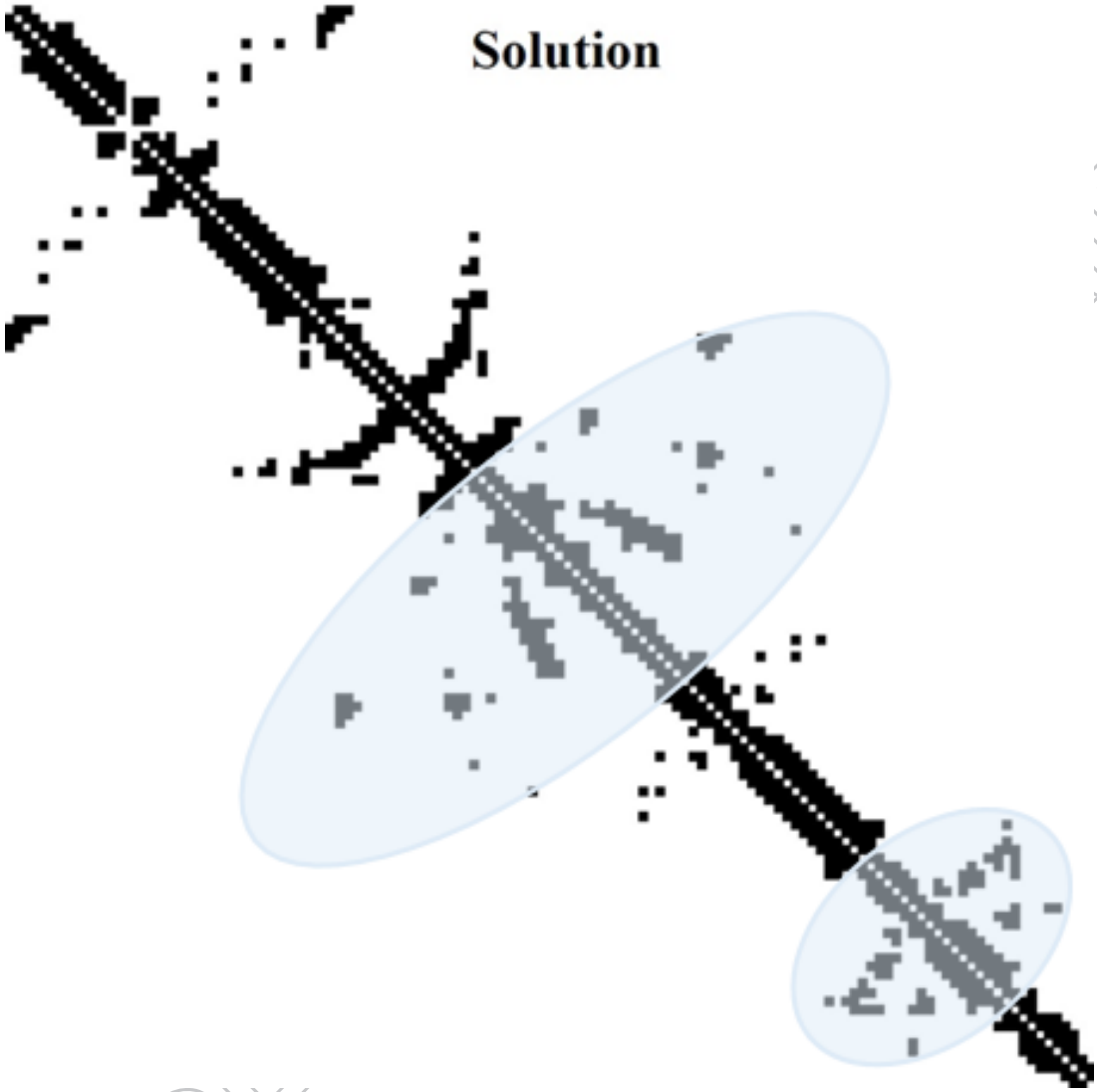
Solution

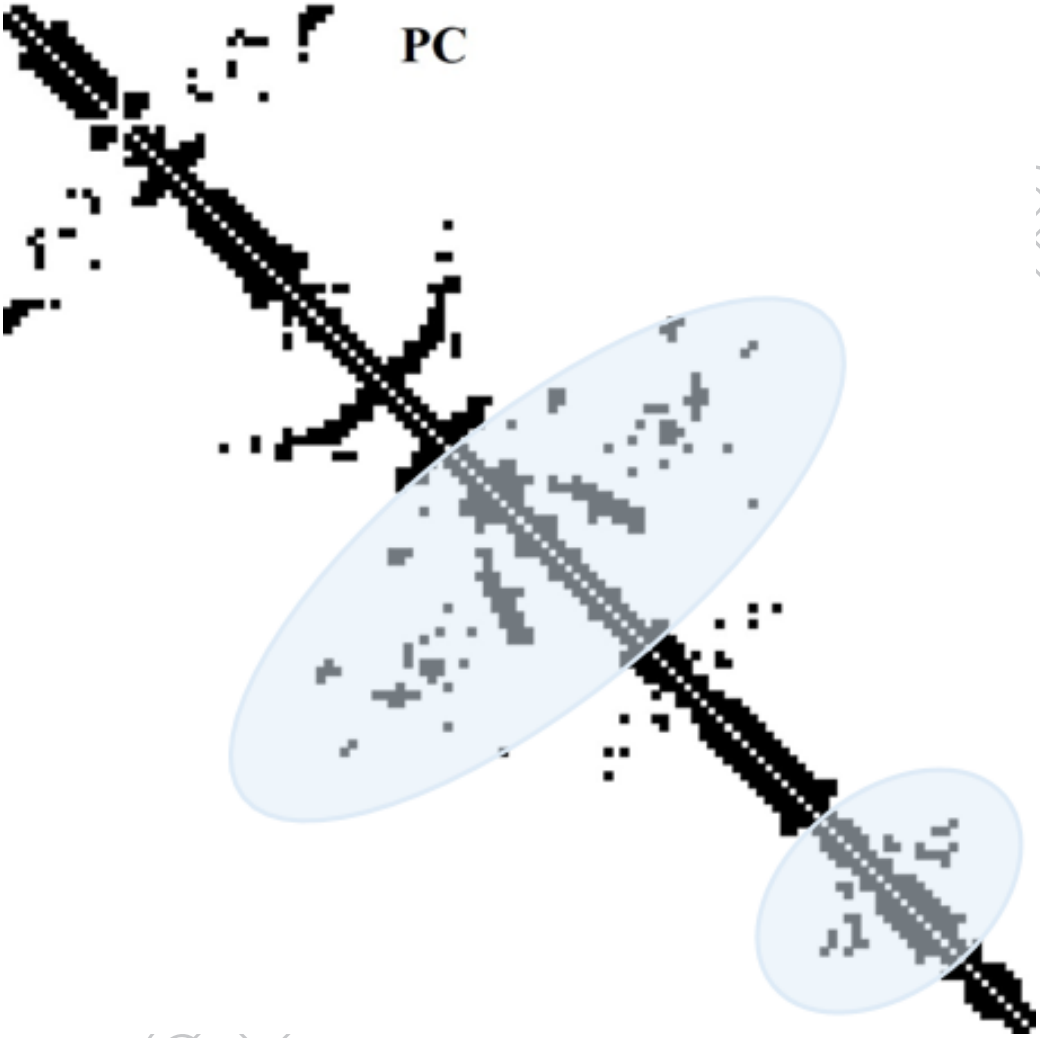
PC